Molecular Vision 2017; 23:624-637 <http://www.molvis.org/molvis/v23/624>
Received 14 October 2015 | Accepted 31 August 2017 | Published 1 September 2017

A novel truncation mutation in *CRYBB1* associated with autosomal dominant congenital cataract with nystagmus

Yan Rao,[1] Sufang Dong,[1] Zuhua Li,[1] Guohua Yang,[3] Chunyan Peng,[1] Ming Yan,[2] Fang Zheng[1]

[1]Center for Gene Diagnosis, Zhongnan Hospital of Wuhan University, Wuhan, China; [2]Department of Ophthalmology, Zhongnan Hospital of Wuhan University, Wuhan, China; [3]Department of Medical Genetics, School of Basic Medical Science, Wuhan University, Wuhan, China

Purpose: To identify the potential candidate genes for a large Chinese family with autosomal dominant congenital cataract (ADCC) and nystagmus, and investigate the possible molecular mechanism underlying the role of the candidate genes in cataractogenesis.
Methods: We combined the linkage analysis and direct sequencing for the candidate genes in the linkage regions to identify the causative mutation. The molecular and bio-functional properties of the proteins encoded by the candidate genes was further explored with biophysical and biochemical studies of the recombinant wild-type and mutant proteins.
Results: We identified a c. C749T (p.Q227X) transversion in exon 6 of *CRYBB1*, a cataract-causative gene. This nonsense mutation changes a phylogenetically conserved glutamine to a stop codon and is predicted to truncate the C-terminus of the wild-type protein by 26 amino acids. Comparison of the biophysical and biochemical properties of the recombinant full-length and truncated βB1-crystallins revealed that the mutation led to the insolubility and the phase separation phenomenon of the truncated protein with a changed conformation. Meanwhile, the thermal stability of the truncated βB1-crystallin was significantly decreased, and the mutation diminished the chaperoning ability of αA-crystallin with the mutant under heating stress.
Conclusions: Our findings highlight the importance of the C-terminus in βB1-crystallin in maintaining the crystalline function and stability, and provide a novel insight into the molecular mechanism underlying the pathogenesis of human autosomal dominant congenital cataract.

Cataract can be defined as any opacity or cloudiness of the crystalline lens resulting from a variation in the refractive index of the lens [1]. Congenital cataract, one of the leading causes of treatable blindness worldwide, has a prevalence of 1–15/10,000 live births with a greater presence in developing countries than in developed countries [2,3]. Congenital cataract is a clinically and genetically heterogeneous disease. Hereditary cataracts usually account for between 8.3% and 25% of congenital cataracts [1,4]. Congenital cataract can be inherited as one of three patterns: autosomal dominant (AD), autosomal recessive (AR), or X-linked transmission, with autosomal dominant the most prevalent form of inheritance pattern [5,6]. To date, about 35 genes have been strongly associated with inherited cataract only and without other systemic anomalies [7]. Of the disease-causing mutations reported, about half are located in crystallins, 15% in connexins, 10% in transcription factors, 5% each in intermediate filaments or aquaporin 0, and 10% in a variety of other genes [5]. Crystallin genes encode more than 95% of the water-soluble structural proteins present in the vertebrate crystalline lens and are divided into two major classes, the α-crystallin family and the β/γ-crystallin superfamily [8]. The α-crystallins are small heat shock proteins that function as molecular chaperones. The β- and γ-crystallins share a common structural feature consisting of four Greek key motifs (GKMs). The major sequence difference between oligomeric β-crystallins and monomeric γ-crystallins is that β-crystallins have long-terminal extensions that are important for β-crystallin function [9]. Biophysical studies have indicated that the unique spatial arrangement and short-range ordering of the crystallin proteins establish the optical transparency [10] and the high refractive index of the lens [11,12]. However, the molecular mechanisms of congenital cataract caused by the gene mutations of crystallins are still unclear, especially the novel mutations. Functional analysis of these mutants is needed to disclose the underlying pathogenesis of congenital cataract.

In this study, we identified a novel nonsense mutation c. C749T (p.Q227X) in exon 6 of *CRYBB1* (GeneID 1414 OMIM: 600929) that altered a phylogenetically conserved glutamine to a stop codon in a Chinese family with autosomal dominant congenital cataract (ADCC). Biophysical studies of the recombinant wild-type (WT) full-length βB1 and mutant (MU) protein revealed that this mutation resulted in an alteration of the structure, solubility, and stability of the βB1 protein

Correspondence to: Fang Zheng, Zhongnan Hospital, Wuhan University Center for Gene Diagnosis, Zhongnan Hospital, Donghu road 169#, Wuhan, Hubei 430071, China; Phone: 862761155235; FAX: 862767813233; email: zhengfang@whu.edu.cn

and led to a decrease in the ability of αA-crystallin to protect the βB1 protein in the heteromers against aggregation induced by heat stress. To our knowledge, this is a novel mutation of βB1-crystallin found to be disease-causing for congenital nuclear cataracts with nystagmus, and thus, functional studies on this mutation offer new insight into cataractogenesis.

METHODS

Clinical assessment and DNA specimens: A five-generation family with congenital cataract and nystagmus, originating from Hubei province, was recruited at the Department of Ophthalmology, Zhongnan Hospital (Wuhan University, Hubei, China). A total of 24 family members (11 affected and 13 unaffected individuals) participated in this study and had a full ocular assessment to document the phenotype, including visual acuity testing and slit-lamp photography. Informed consent was collected and 2 ml venous blood was obtained by venipuncture into the siliconized vacutainer tubes containing 7.5% EDTA. Genomic DNA was extracted from peripheral venous blood sample by using the QIAamp DNA kit (Qiagen, Valencia, CA) according to the manufacturer's instructions. This study was approved by the Medical Ethics Committee of Zhongnan Hospital of Wuhan University and adhered to the tenets of the Declaration of Helsinki and the study adhered to the ARVO statement on human subjects.

Genotyping and linkage analysis: Exclusion analysis was conducted in all participants with polymorphic microsatellite markers flanking 32 known candidate genes [13] to determine whether all patients share the same allele [14,15]. Then fine mapping was performed using additional polymorphic microsatellite markers that flank the candidate locus. Haplotypes were generated using the program Cyrillic 2.1 (published by Cherwell Scientific publishing Ltd, UK). Two-point linkage analysis was performed using the MLINK program of the LINKAGE software package (version 5.2). The cataract in this family was analyzed as an autosomal dominant trait with full penetrance and a gene frequency of 0.0001. The allele frequencies for each marker were assumed to be equal in both genders.

Mutation and bioinformatics analysis: Genomic DNA samples from the family participants and 100 population controls were extracted. The genomic DNA of the proband was screened for mutations in previously reported ADCC disease-causing genes, including *CRYAA* (Gene ID: 1409, OMIM 123580), *CRYAB* (Gene ID: 3316; OMIM: 602179), *CRYBA1* (Gene ID: 1411, OMIM 123610), *CRYBA4* (Gene ID: 1413, OMIM 123631), *CRYBB1*, *CRYBB2* (Gene ID: 1415, OMIM: 123620), *CRYGC* (Gene ID: 1420, OMIM: 123680), *CRYGD* (Gene ID: 1421, OMIM: 123690), *GJA8* (Gene ID: 2703, OMIM: 600897), *GJA3* (Gene ID: 2700, OMIM: 121015), *MIP* (Gene ID: 4284, OMIM: 154050), and *BFSP2*, (Gene ID: 8419, OMIM: 603212) with direct sequencing. The genomic DNA of the controls was screened for the candidate mutation. Briefly, individual exons and the flanking intron sequences of these candidate genes were amplified with PCR, and then the PCR products were sequenced on an ABI 3730XL Automated Sequencer (PE Biosystems, Foster City, CA) using gene-specific primers as previously described [16]. The cycling conditions for PCR included a denaturation step at 95 °C for 3 min, 10 cycles of touchdown PCR with a 1 °C decrement of the annealing temperature per cycle from 70 °C to 61 °C, then maintained at 60 °C for 20 more cycles. Each cycle consisted of a denaturation at 94 °C, annealing step and extension at 72 °C, all for 30 s, with a final extension at 72 °C for 10 min. Amino acid sequences for βB1-crystalline were retrieved from NCBI. Multiple sequence alignments of βB1-crystalline from various species were performed using DNAMAN software (version 5.0, Lynnon BioSoft, Vaudreuil, Canada). Three-dimensional structures of the WT βB1 and the mutant were modeled employing the Swiss Model server program (provided in collaboration by the Biozentrum of University of Basel, the Swiss Institute of Bioinformatics, and the NCI Advanced Biomedical Computing Center). The resulting protein database files were visualized using Swiss-sPdb Viewer (version 4.01, provided by Swiss Institute of Bioinformatics, Geneva, Switzerland).

Molecular cloning of CRYBB1 and CRYAA recombinants: The total cDNA of the human lens was obtained using the standard methods as described elsewhere [17]. The coding sequences of *CRYBB1* and *CRYAA* were isolated from the human lens cDNA with PCR using the following primers: WT *CRYBB1* primers (F: 5′-GGA ATT CCA TAT GAT GTC TCA GGC TGC AAA GGC CT-3′, R: 5′-CGC GGA TCC TCA CTT GGG GGG CTC TGT GG-3′) and *CRYAA* primers (F: 5′-AAT CCA TGG ACA TCG CCA TCC ACC-3′, R: 5′-TAC CTC GAG TTT CTT GGG GGC TGC-3′). The sense and anti-sense primers for the construction of the MU *CRYBB1* were 5′-GGA ATT CCA TAT GAT TCT CAG GCT GCA AAG GCC T-3′ and 5′-CGC GGA TCC CTA CAT CTG TGG CTG GAA GGC TCC-3′, respectively. The PCR product was cloned in a T-simple vector (Takara, Beijing, China) and sequenced. For protein expression, the coding sequences of *CRYBB1* and *CRYAA* were then inserted between the NdeI/BamHI sites and the NcoI&XhoI sites, respectively, in pET28a vectors for the expression constructs.

Protein expression and purification: The procedure details regarding the overexpression and purification of the recombinant proteins were followed as previously described with

minor modifications [16]. Briefly, *Escherichia coli* BL21 (DE3) was transformed with expression constructs using a standard *E. coli* transformation procedure. The proteins were overexpressed by the addition of isopropyl β-D-1-thiogalactopyranoside (IPTG, final concentration of 0.1 mM) when the cell cultures reached an optical density (OD) value of 0.6, and the cultures were incubated further at 37 °C for 4 h. The cells were harvested, resuspended in lysis buffer (20 mM sodium phosphate, 0.5 M NaCl, 1% phenylmethanesulfonyl fluoride, PMSF), and lysed by sonication in an ice bath. The soluble fraction was separated by centrifugation at 8,000 ×*g* for 30 min at 4 °C, and the pellet was resuspended in a detergent buffer (0.02 M Tris-HCl, pH 7.4, containing 1% (w/v) sodium deoxycholate, 0.2 M NaCl, and 1% NP-40) and centrifuged at 5,000 ×*g* for 10 min at 4 °C. The pellet was washed with 0.5% Triton X-100 and then was resuspended in denaturation buffer (20 mM sodium phosphate buffer, pH 7.4, containing 8 M urea and 0.5 M NaCl). Depending on the expression of the desired proteins in the soluble fraction or the inclusion bodies, the proteins were purified under either native or denaturing conditions [18,19]. The recombinant proteins containing six His-tags at the N-terminus were purified with an affinity chromatographic method using the Ni^{2+} chelating column. During the purification process under native conditions, a column was equilibrated with the native buffer (20 mM sodium phosphate buffer (pH 7.4) containing 0.5 M NaCl) at first. Then, the protein preparation was applied to the column and washed with a native buffer containing 10 mM imidazole, and finally, the matrix-bound protein was eluted with a native buffer containing 250 mM imidazole (pH 7.4). However, during purification of the mutant protein under denaturing conditions, the column was equilibrated with a denaturation buffer at first. Following the protein application, the unbound proteins were eluted, first with a denaturation buffer, which was followed by a second wash with a denaturation buffer at pH 6.0 and a third wash with denaturation buffer at pH 5.3. The bound proteins were eluted with denaturation buffer containing 250 mM imidazole (pH 7.4). The sodium dodecyl sulfate–polyacrylamide gel electrophoresis (SDS–PAGE) analysis was used to identify the fractions that contained the desired proteins during purification. The protein purified under native conditions was pooled, dialyzed against 50 mM phosphate buffer (pH 7.4) at 4 °C, and stored at −80 °C until used. The denatured mutant protein was refolded in a urea-free buffer under denaturing conditions following a method described elsewhere [19]. Briefly, the mutant protein was refolded by adding it dropwise to an excess of cold buffer (25 mM Tris-HCl, 1 mM DTT, pH 7.5) at 1:100 dilution (denatured protein:buffer). The protein concentrations were determined using a Pierce Coomassie Plus Assay Reagent (Pierce Chemical, Rockford, IL) according to the Bradford method.

Circular dichroism studies: The circular dichroism (CD) spectra were obtained with a Model J-810 spectropolarimeter (Jasco, Tokyo, Japan). WT and MU βB1 protein solutions at 0.2 mg/ml (dissolved in 50 mM sodium phosphate buffer, pH 7.4) were used to record the CD spectra. The spectra reported were the average of five scans, corrected for buffer blank, and smoothed. The CD data were expressed as the molar ellipticity in degrees cm^2/dmol.

Fluorescence spectroscopy: All fluorescence measurements were performed using a Hitachi F-4500 FL spectrophotometer (Hitachi, Tokyo, Japan) with a protein concentration of 0.2 mg/ml at room temperature. The excitation and emission band passes were set at 5 and 3 nm, respectively. The intrinsic Trp fluorescence intensities of the WT and truncated MU βB1 proteins dissolved in 50 mM sodium phosphate buffer (containing 100 mM NaCl, pH 7.4) were recorded with an excitation at 280 nm and an emission between 300 and 400 nm. The extrinsic 8-anilinonaphthalene-1-sulfonic acid (ANS) fluorescence spectra were recorded at wavelengths ranging from 400 to 600 nm with the excitation wavelength at 380 nm. Fluorescence intensity was then measured, and the readings were corrected for buffer blanks. In the ANS fluorescence experiments, 15 µl of 0.8 mM ANS (dissolved in methanol) was added to the purified WT and MU βB1 protein solutions (0.2 mg/ml, dissolved in 50 mM phosphate buffer, pH 7.4).

Size exclusion chromatography: Size determinations of the oligomeric βB1 protein in solution were performed using gel filtration chromatography (size exclusion chromatography, SEC) with an OHpak SB-804 HQ column (Shodex, Tokyo, Japan) equilibrated in 50 mM sodium phosphate (pH 7.4) containing 100 mM NaCl [20]. The concentrations of the full length and truncated βB1 proteins were adjusted to the same concentration of 0.5 mg/ml, and 100 µl of each sample solution was applied to the column. The flow rate was 0.5 ml/min.

Phase separation: Solutions of recombinant WT and MU βB1 proteins at a concentration of 1.5 mg/ml in 50 mM sodium phosphate (pH 7.4) were examined for their ability to undergo reversible cryoprecipitation or phase separation. The initial concentrations of the solutions were determined after they had been spun down at 13,000 ×g at 20 °C for 5 min, by measuring the absorption of the dilution of 5 µl supernatant at 280 nm that diluted into 370 µl of sodium phosphate at pH 7.4. The protein solutions were then placed at 4 °C for 1 h before they were spun down at 13,000 ×g at 4 °C for 5 min. The protein concentration in the supernatant was determined as above. Then, the solutions were allowed to return to room

temperature, and the supernatant was determined again to verify the reversibility of the process.

Light scattering: Light scattering was determined indirectly by measuring absorbance at 405 nm. Based on previous reports, a βB1 protein solution with the concentration of 0.2 mg/ml contained predominantly monomers of βB1, while solutions with higher concentrations were predominantly dimers with small amounts of higher-ordered oligomers [21]. The samples at 0.1 mg/ml were heated at 55 °C for 750 min in a thermal jacketed cuvette with constant stirring (Cary 4 Bio UV-Visible spectrophotometer, Varian, Palo Alto, CA). Incubations were performed in the same buffer as that in CD detection. The WT βB1 protein was heated at 55 °C alone or with an equal molar amount of αA-crystallin, and the results were compared with those resulting from heating the MU βB1 protein alone or with an equal molar amount of αA-crystallin.

RESULTS

Clinical findings: We identified a five-generation Chinese family with a clear diagnosis of congenital cataract with 24 living members (Figure 1A). According to the history and medical records, all affected individuals showed bilateral nuclear cataracts of variable severity before the age of 5. They had similar poor visual acuity and nystagmus without other ocular or systemic abnormalities (Figure 1B,C). Clinical features of cataract were symmetric in two eyes of most affected individuals. The details about the phenotypes of the affected individuals are presented in Table 1. The pedigree of the family suggests an AD mode of inheritance.

Linkage and mutation analysis identified a nonsense mutation: Allele-sharing analysis excluded all the known cataract-related loci except the β-crystallin cluster on chromosome 22q11.2–12.1. Linkage analysis gave a maximum two-point logarithm (base 10) of odds (LOD) score of 2.69 for marker D22S283 at recombination fraction [θ] = 0 (Appendix 1). Haplotype analysis showed that the affected individuals in the family shared a common haplotype between D22S277 and D22S283 (Figure 1A). These markers closely flank the *CRYBB3*, *CRYBB2*, *CRYBB1*, and *CRYBA4* gene cluster. Meantime, direct sequencing of the coding regions and the flanking intronic sequences of previously reported ADCC disease-causing genes (*CRYAA*, *CRYAB*, *CRYBA1*, *CRYBA4*, *CRYBB1*, *CRYBB2*, *CRYGC*, *CRYGD*, *GJA8*, *GJA3*, *MIP*, and *BFSP2*) in the proband revealed no nucleotide changes except a heterozygous c. C749T (p.Q227X) transition in exon 6 of *CRYBB1* and a synonymous single nucleotide variation in *CRYAA* (the C/T transition). The synonymous C/T variation in *CRYAA* (rs872331) identified in the proband was a known polymorphism. The nonsense mutation changed a phylogenetically conserved glutamine to a stop codon that was cosegregated with all affected individuals in the family (Figure 1E). In addition, this single nucleotide change was not detected in any of the unaffected family members or the 100 healthy unrelated individuals from the same ethnic background. It suggested that this mutation was the causative mutation rather than a rare polymorphism in strong linkage disequilibrium with the disease in this pedigree. Multiple sequence alignments generated using DNAMAN software showed that the Gln residue at position 227 of human βB1-crystallin was highly conserved in *Mus musculus*, *Rattus norvegicus*, *Bos taurus*, *Cavia porcellus*, *Gallus gallus*, *Danio rerio*, and *Xenopus tropicalis* (Figure 2B). This nonsense mutation led to a truncated protein with the deletion of the C-terminal extension plus partial motif IV and conformational changes in the βB1-crystallin (Figure 2A–D).

Recombinant βB1 proteins and αA-crystallin were expressed and purified: After expression in *E. coli*, the WT βB1 and αA-crystallins were recovered in the soluble fractions, whereas the MU βB1-crystallin was exclusively present in the insoluble inclusion body fractions (Figure 2E). The WT βB1- and αA-crystallins present in the soluble fractions were purified under native conditions, and the MU βB1-crystallin that was present in the insoluble fractions was purified under denaturing conditions. The purified proteins on SDS–PAGE analysis showed a single major protein band suggesting their highly purified nature (Figure 2F).

Effect of the p.Q227X mutation on the structure βB1-crystallin: To evaluate the effects of p.Q227X mutation of βB1-crystallin on the structural properties, far-ultraviolet (UV) CD and intrinsic Trp fluorescence of the WT and MU βB1-crystallins were determined (Figure 3A). The far-UV CD spectra indicated that the p.Q227X mutation slightly decreased the mean residue ellipticity of βB1-crystallin, suggesting that the mutation led to a minor decrease in the percentages of the regular secondary structure. The deletion of the C-terminal extension plus partial motif IV resulted in an approximate 1 nm red shift in E_{max} and increased intrinsic Trp fluorescence. The results suggested that the mutation slightly modified the tertiary structures of the truncated mutant, which further influenced the populations and exposure of the remaining Trp fluorophores.

To investigate the effects of truncation on surface hydrophobicity of the proteins, the extrinsic fluorescence probe ANS binding to the WT and MU βB1 proteins was detected (Figure 3C). The truncated mutation increased the ANS fluorescence intensity of the βB1 protein by almost 10%. The results showed that the truncated mutant had more

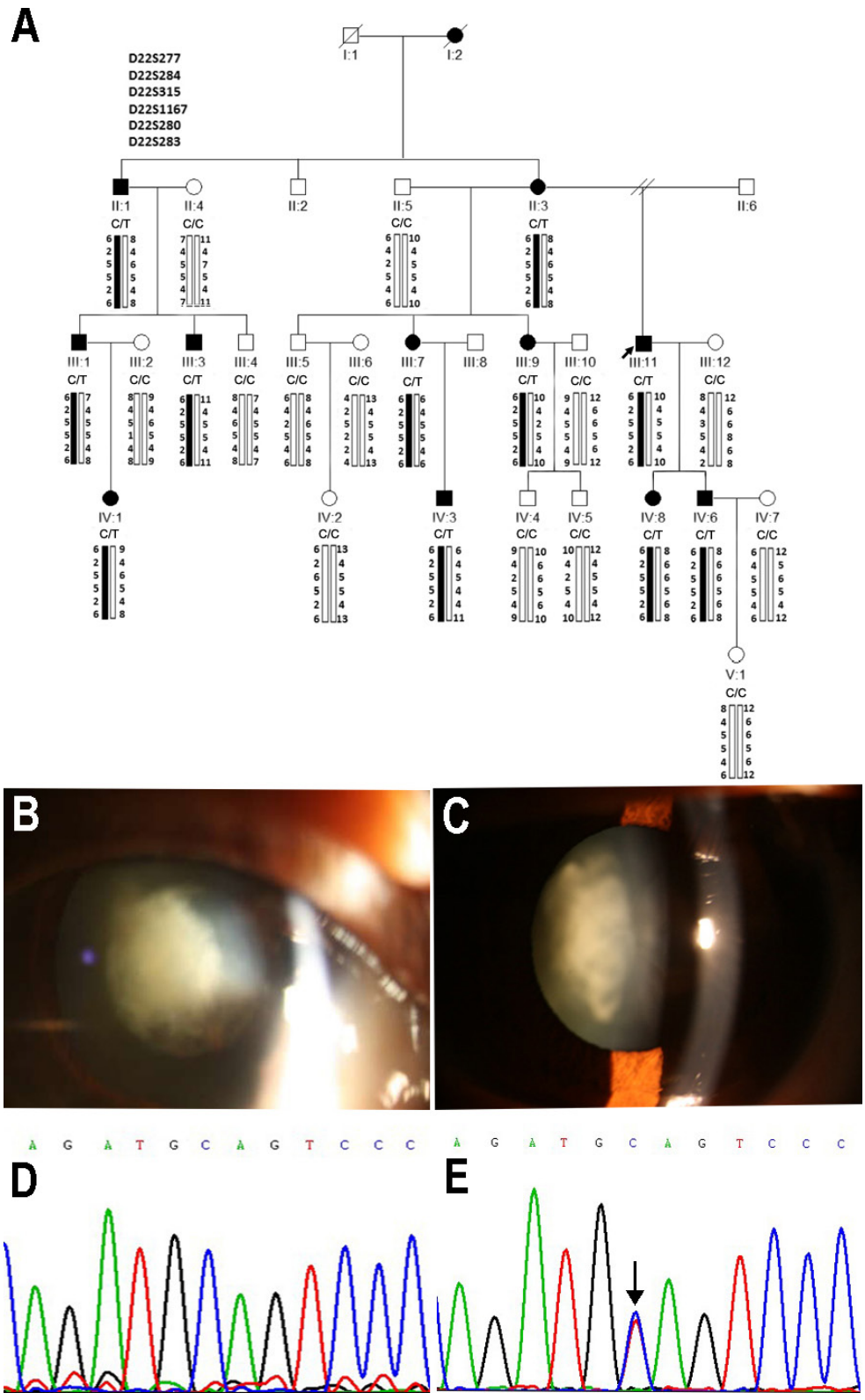

Figure 1. Mutation analysis of *CRYBB1* in a Chinese family with congenital cataract. **A**: Pedigree and haplotype analysis of the family showing the segregation of six microsatellite markers on chromosome 22q11.2–12.1. Squares and circles indicate men and women, respectively. Solid symbols and bars denote affected status. The proband is indicated with an arrow. C/C and C/T indicate the *CRYBB1* genotypes. **B**: Front view of the eye of the proband, showing dense nuclear opacities with nystagmus. **C**: Slit-lamp view of the lens of the proband. Lens opacities are mainly located in the nuclear area of the lenses, as well as in the embryonal and fetal areas. **D**, **E**: Sequence chromatograms of one unaffected individual (**D**) and one affected individual (**E**) of exon 6 of the *CRYBB1* gene in this family with autosomal dominant congenital cataract (ADCC). The DNA sequence chromatogram shows a c. 749 C>T heterozygous mutation in *CRYBB1* indicated by an arrow in panel **E**.

Table 1. Clinical characteristics of a Chinese pedigree with autosomal dominant congenital cataracts in our study.

Pedigree number	Gender	Age (years)	Genotype	Base on db protein (NP_005258.2)	Phenotype (LOCS 3 scale)
II:1	M	62	C/T	p.Q227X	N4C4P3Nc4
II:3	F	68	C/T	p.Q227X	N4C4P3Nc4
II:4	F	60	C/C		Normal
II:5	M	70	C/C		Normal
III:1	M	42	C/T	p.Q227X	N3C3P3Nc3
III:2	F	38	C/C		Normal
III:3	M	40	C/T	p.Q227X	N3C4P3Nc3
III:4	M	36	C/C		Normal
III:5	M	40	C/C		Normal
III:6	F	38	C/C		Normal
III:7	F	43	C/T	p.Q227X	N3C3P3Nc3
III:9	F	45	C/T	p.Q227X	N3C3P3Nc3
III:10	M	44	C/C		Normal
III:11	M	47	C/T	p.Q227X	N3C4P3Nc3
III:12	F	43	C/C		Normal
IV:1	F	16	C/T	p.Q227X	N0C2P0Nc0.6
IV:2	F	18	C/C		Normal
IV:3	M	20	C/T	p.Q227X	N0C2P0Nc0.3
IV:4	M	23	C/C		Normal
IV:5	M	21	C/C		Normal
IV:6	M	23	C/T	p.Q227X	N0C3P1Nc1
IV:7	F	22	C/C		Normal
IV:8	F	26	C/T	p.Q227X	N0C2P1Nc0.4
V:1	F	2	C/C		Normal

ANS-accessible sites and resulted in increased exposure of hydrophobic patches.

Truncation had less effect on the oligomeric size: Previous studies showed that the N-terminal region of the crystallin controlled the degree of oligomerization [22,23]. Here, SEC was performed to determine the oligomeric size of the recombinant βB1 protein and to ascertain whether the C-terminal deletion influenced oligomerization. As shown in Figure 3D, the average retention times for the WT and MU βB1 proteins were similar. The data indicated that the oligomeric size of the recombinant WT and MU βB1 proteins was not significantly different, which was consistent with the findings that the C-terminal extension has less effect on controlling the oligomeric size of the βB1 protein compared with the N-terminal region [24].

Truncated βB1 protein was prone to phase separation: The solutions of the WT and MU βB1 proteins remained clear after standing at 37 °C for 1 h. However, the solution of the MU βB1 protein was completely opaque after only 15 min at 4 °C and produced a significant white pellet when spun down. The concentration of the supernatant solutions of the WT βB1 protein after centrifugation had little change while the concentration of the supernatant of the solution of the MU βB1 protein decreased by 25%. The pellet of the MU βB1 protein failed to redissolve effectively when brought back to 25 °C.

Effect of the p.Q227X mutation on the thermal stability: As a measure of unfolding and aggregation, changes in absorbance due to light scattering at 405 nm were followed for dilute solutions of the WT and MU βB1 proteins (0.1 mg/ml) upon heating at 55 °C (Figure 4). The truncated mutant protein showed a significantly greater increase in light scattering due to protein aggregation, demonstrating lower thermal stability.

The chaperoning ability of αA-crystallin with the βB1 protein: Meanwhile, the ability of αA-crystallin to prevent, via its chaperone action, the aggregation of the βB1 protein

upon heating was also tested. The presence of the 1:1 molar ratio of αA-crystallin to the WT βB1 protein significantly diminished the increase in light scattering after the WT βB1 was heated. In contrast, the αA-crystallin could partially stabilize the truncated MU βB1 protein, but the efficiency of chaperoning MU βB1 was much weaker compared to that of the WT βB1 protein (Figure 4). These results suggested that the C-terminal extension played an important role in keeping the solubility and stability of the βB1 protein, even under the status of cooling or heating stress.

DISCUSSION

In this study, we identified a novel nonsense mutation c. C749T (p.Q227X) in exon 6 of *CRYBB1* that is the causative gene for ADCC in a five-generation Chinese family. This mutation led to a chain-termination at codon 227 in the GKM IV and was predicted to truncate the full-length βB1 protein by 26 amino acids. The truncated βB1 protein became water insoluble with the deletion of its C-terminal extension and partial GKM IV. The truncation also resulted in alteration in the conformation and characteristics of phase separation. Furthermore, the truncation reduced the thermal stability of the βB1 protein and weakened the chaperoning ability of αA-crystallin with the βB1 protein under heating stress.

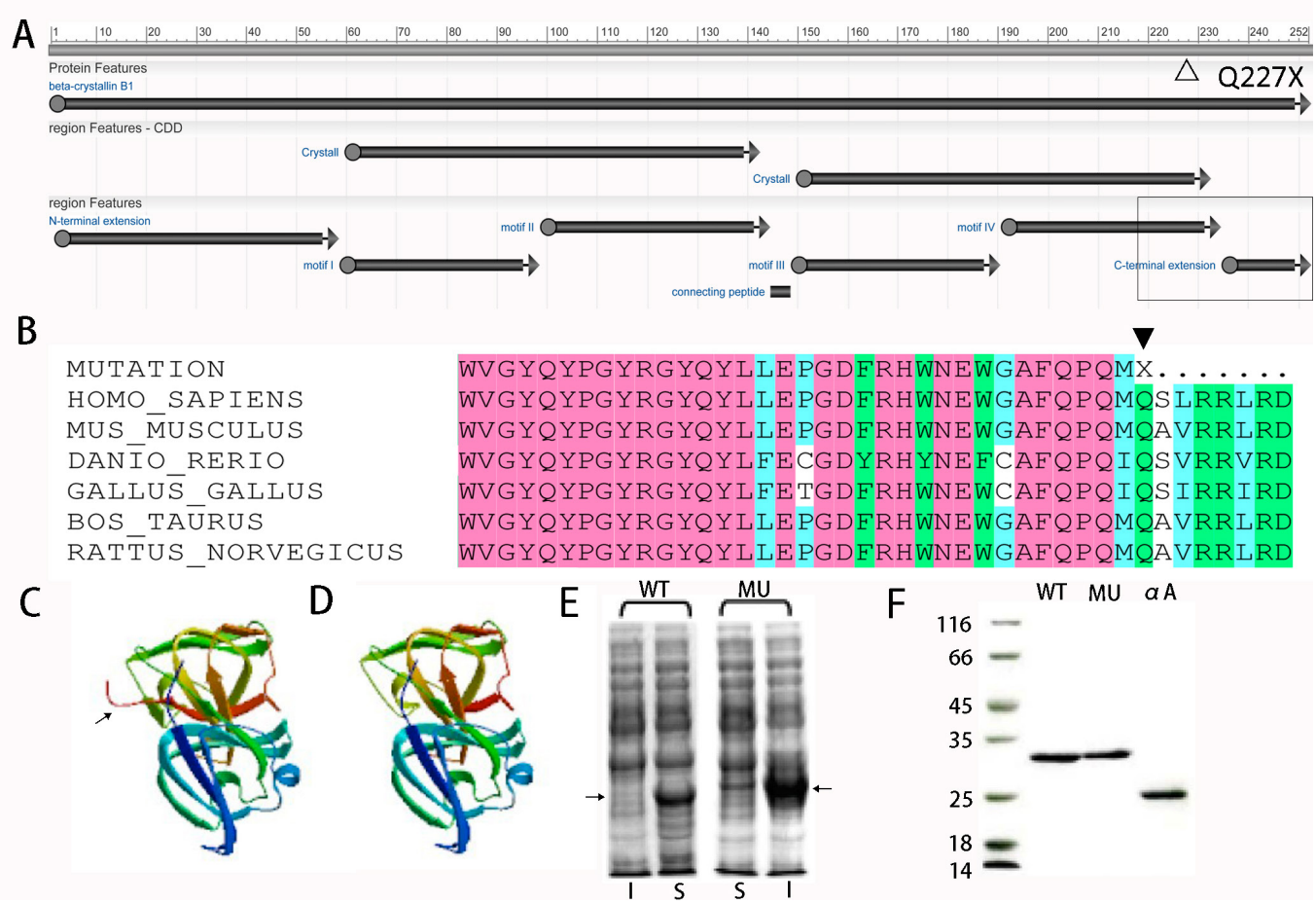

Figure 2. Comparison between the structure and solubility of WT and MU-βB1 proteins. **A**: Diagrammatic sketch of βB1 protein features. The hollow triangle indicates the position of p.Q227X; the hollow rectangle indicates the truncated partial motif VI and C-terminus. **B**: Multiple-sequence alignment of βB1-crystallin. The Gln227 residue is highly conserved during evolution shown with a solid triangle. **C**: The predicted tertiary structure of wild-type (WT) βB1-crystallin. **D**: The predicted tertiary structure of mutated βB1-crystallin. The C-terminus of the wild-type protein is pointed by an arrow, which disappeared in the mutant. **E**: Distribution of the recombinant expression of the WT and mutant (MU) βB1 proteins in the *Escherichia coli* (DE3) strain. I = inclusion bodies; S = supernatant; the arrow indicates the WT or MU βB1 proteins. **F**: Sodium dodecyl sulfate–polyacrylamide gel electrophoresis (SDS–PAGE) analysis of purified WT-βB1, its truncation mutant (MU-βB1), and αA-crystallin. Lanes: WT, WT-βB1; MU, MU-βB1; αA, αA-crystallin.

The *CRYBB1* gene encodes a 252-amino acid protein mainly expressed in the early lens nucleus. βB1-crystallin, a major subunit of the beta-crystallins, comprises 9% of the total soluble crystallins in human lens, and the amount decreases dramatically with age. βB1-crystallin is thought to be important for the maintenance of lens transparency. Mackay et al. mapped the pathogenic gene of the dominant pulverulent cataract to the *CRYBB1* gene on chromosome 22q12.1 and found that the p.G220X mutation in this gene was responsible for ADCC [25]. To date, at least ten mutations in *CRYBB1* have been identified in families with inherited cataract and some additional developmental ocular abnormalities (Table 2). Five mutations (p.G220X, p.Q223X, p.S228P, p.R233H, and p. X253R) are located in exon 6 of the *CRYBB1* gene [9,14,25-27], which indicates that the exon 6 that encodes the COOH terminal domain and the GKM IV is the hot site for mutations. All five families inherited as an AD trait and revealed a nuclear cataract phenotype with or without other ocular abnormalities, such as microcornea and nystagmus. The p.R123H and p.S129R mutations located in exon 4 that encodes the GKM II were also cosegregated with autosomal dominant nuclear cataract [28,29]. Reis et al. reported a p.V96F mutation located in exon 3 in a dominant congenital cataract with glaucoma and microcornea [30].

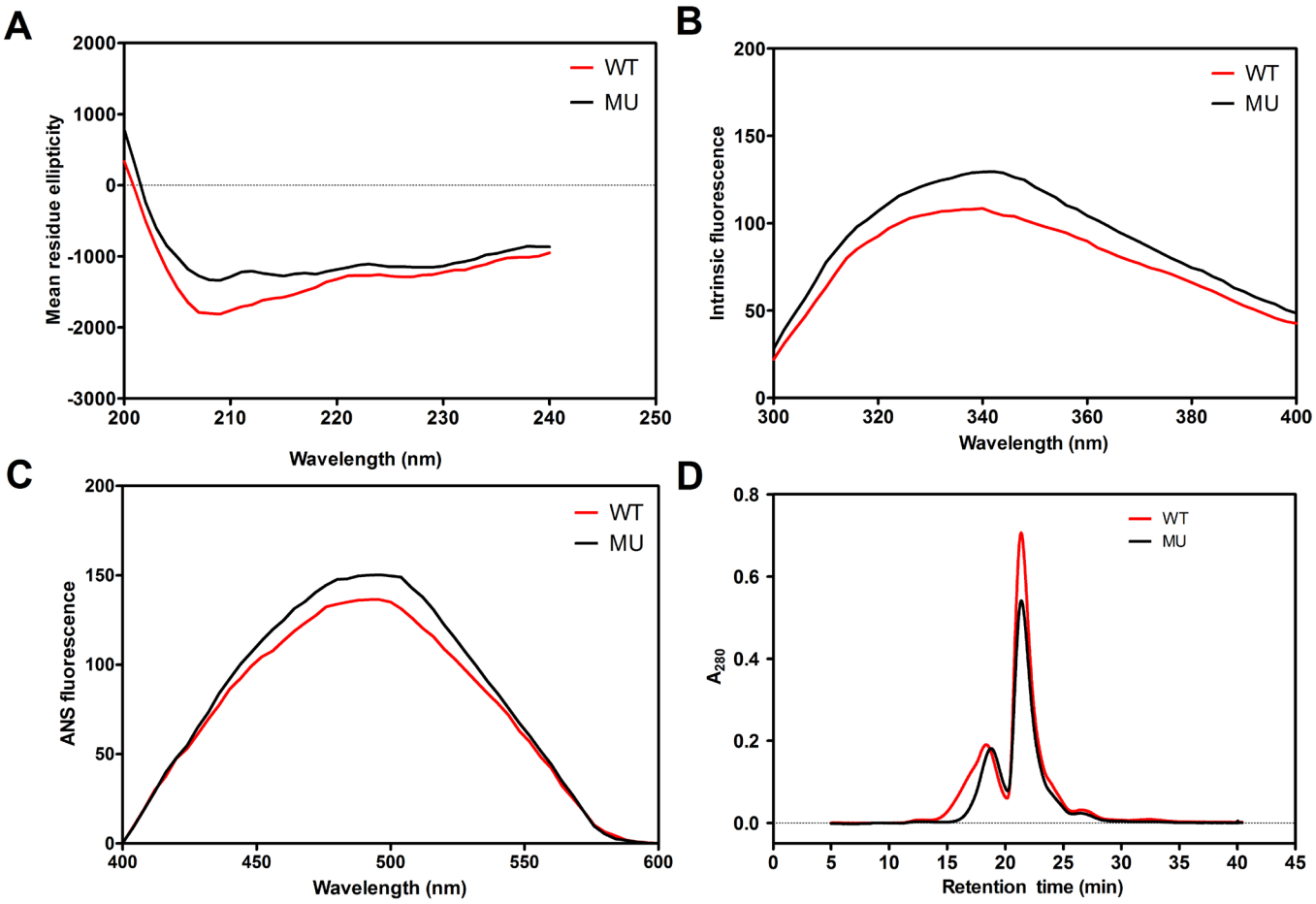

Figure 3. Biophysical characterization of the effect of the mutation in p.Q227X on the structures of βB1-crystallin. **A**: Far-ultraviolet (UV) circular dichroism (CD) spectra of the wild-type (WT) βB1 protein and its mutant protein. The spectra were determined at room temperature using a JASCO spectropolarimeter, model J-810. The βB1-crystallin preparations at 0.5 mg/ml (50 mM sodium phosphate buffer, pH 7.4) were used to record the far-UV CD spectra. The path length was 0.1 cm during the far-UV CD spectra determination. The spectra reported were the average of five scans, corrected for buffer blank, and were smoothed. **B**: Intrinsic Trp fluorescence intensities of the WT-βB1 protein and its mutants. The proteins (0.2 mg/ml each) were dissolved in 50 mM sodium phosphate buffer, pH 7.4, containing 100 mM NaCl, and were recorded with an excitation at 280 nm and emission between 300 and 400 nm. **C**: Binding of 8-anilinonaphthalene-1-sulfonic acid (ANS) to the WT βB1 and mutant proteins. In these experiments, 15 µl of 0.8 mM ANS (dissolved in methanol) was added to a protein preparation (0.2 mg/ml, dissolved in 50 mM phosphate buffer, pH 7.4). The samples were incubated at 37 °C for 15 min before the fluorescence spectra were recorded after excitation at 380 nm and emission between 400 and 600 nm. **D**: Gel filtration chromatography of the WT βB1 and mutant (MU) βB1 proteins performed on an OHpak SB-804 HQ column.

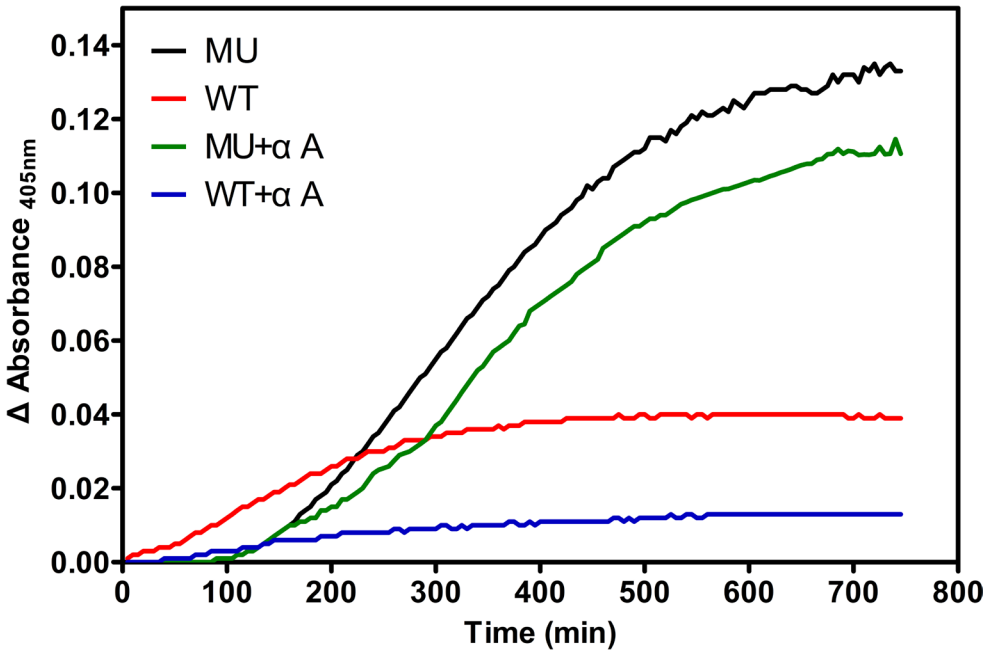

Figure 4. Thermal denaturation of WT and MU βB1 monomers and heteromers with αA-crystallin. Thermal denaturation curves were obtained by heating 0.2 mg/ml of the wild-type (WT) and mutant (MU) βB1 proteins at 55 °C in a 50 mM phosphate buffer, pH 7.4, and then measuring light scattering at 405 nm. Meanwhile, the WT βB1 protein was heated at 55 °C with an equal molar amount of αA-crystallin, and the results were compared with those for heating the MU βB1 protein with an equal molar amount of αA-crystallin.

However, other mutations located in exon 1 and exon 2 were inherited in a recessive model without other ocular abnormalities [31,32]. Whether this indicated that the mutations closer to the C-terminus would induce more severe phenotypes requires further exploration. However, little functional importance of the mutants was illustrated in the previous few reports, in which the molecular mechanisms demonstrated were most often attributed to disturbance in solubility and stability of βB1-crystallin.

The p.Q227X mutation described in the present study is a nonsense mutation of *CRYBB1*, which leads to a truncated protein responsible for bilateral dense nuclear cataract and nystagmus. Likewise, the nonsense mutations located in other crystalline genes were also reported to be associated with congenital cataract (Appendix 2). Pras et al. identified a p.W9X nonsense mutation in the *CRYAA* gene that caused autosomal recessive cataract in one Israelite family [33]. Devi et al. screened the candidate genes in 60 south Indian families and identified a nonsense mutation (*CRYBB2* p.Q155X) responsible for the inherited pediatric cataract [34]. To date, about 22 mutations in *CRYGD* have been reported to be responsible for cataracts, ten of which are nonsense mutations (Appendix 2) [30,34-41]. γD-crystallin is composed of two individual domains that each consist of two GKMs, which is similar to βB1-crystallin. All the nonsense mutations are distributed in the four GKMs. The nonsense mutations p.Y17X and p.Y56X are located in GKMs I and II of the same domain. The nonsense mutations (p.Q101X, p.E104fsX4, p.Y134X, p.E135X, p.R140X, p.Y151X, p.W157X, and p.G165AfsX3) are located in the another domain. Intriguingly, the truncated mutations are mainly in the GKM IV of the C-terminus (6/10). In addition, five nonsense mutations in *CRYGC* have been associated with cataracts, including nuclear cataract with obvious nystagmus (p.C109X) [42], sporadic congenital nuclear cataracts (p.Q113X and p.Y134X) [43,44], nuclear cataracts with other ocular abnormalities, such as microphthalmia, microcornea, glaucoma, and corneal opacity (p.Y139X) [30], nuclear cataracts, and microcornea (p.W157X) [45,46]. In a manner similar to the nuclear opacities associated with the p.Q227X mutation of *CRYBB1* in the present study, nearly all these *CRYGC*-related opacities involve the nucleus of the lens. This clinical manifestation is in agreement that CRYGC and CRYBB1 are abundantly expressed at an early developmental stage in elongating fiber cells. The γC-crystallin and βB1-crystallin are expressed primarily in the lens nucleus, which is consistent with the location of the opacity in the nucleus. The difference in the effects of the clinical features generated by these nonsense mutations is likely to be due to whether they are subjected to nonsense-mediated decay (NMD) [47,48]. NMD alters the patterns of inheritance for premature truncation alleles in many genes with 5′- nonsense mutations (predicted to be subject to NMD) resulting in recessive diseases and 3′-nonsense mutations (predicted to escape NMD) leading to dominant diseases. In terms of cataract genes, examples include mutations in *CRYBB1* with dominant changes comprising missense mutations in the GKM II or IV, the

Table 2. The reported mutations in the *CRYBB1* gene.

Gene	Exon/ Intron	DNA Change	Coding Change	Inheritance	Origin	Cataract Phenotype	Other Phenotype	Ref.
CRYBB1	Ex1	c.2T>A	p.M1K	AR	Somalia	Nuclear, pulverulent		[32]
CRYBB1	Ex2	c.171delG	p.G57GfsX107 (p.N58TfsX106)	AR	Israel	Nuclear		[13]
CRYBB1	Ex2	c.171delG	p.N58TfsX106	AR	Arabian	Pulverulent		[31]
CRYBB1	Ex3	c.286G>T	p.V96F	AD	USA	congenital	Glaucoma, microcornea	[30]
CRYBB1	Ex4	c.368G>A	p.R123H	AD	Australia			[29]
CRYBB1	Ex4	c.387C>A	p.S129R	AD	China	Nuclear	Microcornea	[28]
CRYBB1	Ex6	c.658G>T	p.G220X	AD	Portland	Nuclear progressive		[22]
CRYBB1	Ex6	c.667C>T	p.Q223X	AD	China	Nuclear progressive		[27]
CRYBB1	Ex6	c.682T>C	p.S228P	AD	China	Nuclear	Nystagmus	[14]
CRYBB1	Ex6	c.698G>A	p.R233H	AD	China	Nuclear	Nystagmus	[26]
CRYBB1	Ex6	c.757T>C	p.X253RextX27	AD	UK	Nuclear Cortical riders	Microcornea	[9]

C-terminal extension mutation, and C-terminal truncations that retain about 90% of normal protein sequences but lack part of the GKM IV (all located in exon 6 of *CRYBB1* and predicted to escape NMD). All of these changes are likely to result in the expression of mutant protein, and the p.Q227X mutation in this report is also predicted to escape NMD and express the mutant βB1-crystallin. The truncated mutant might not only induce haploinsufficiency but also get new functions to impair the normal protein interactions. In contrast, the early frameshift mutation and an initiation codon substitution in *CRYBB1* tend to be inherited as a recessive trait and subject to NMD, resulting in null alleles.

In this study, the possible molecular mechanism underlying ADCC with nystagmus caused by the p.Q227X mutation was investigated by comparing the biophysical properties of the recombinant WT and MU βB1 proteins. Consistent with the truncated mutations established in the GKM IV and the C-terminal extension by Srivastava et al., which resulted in a significant change in the solubility of the βB1 protein [19], we found that the p.Q227X mutation dramatically affected the folding of the recombinant βB1 protein in *E. coli*, implying that this novel mutation might undergo molecular mechanisms similar to previously identified ones [19,25,46,49].

First, the insolubility of the p.Q227X mutant containing residues 1–226 further highlights the importance of the intact C-terminal extension in maintenance in the solubility and stability of βB1-crystalline. Second, these results indicated that the mutation slightly modified the secondary and tertiary structures of the truncated βB1 protein and resulted in increased exposure of hydrophobic patches relative to the WT βB1 protein, which was also coincident with the observation of Srivastava's group as well [19]. Moreover, the truncated βB1-crystallin obviously affects the phase separation and thermal stability under the status of cooling or heating stress, as when αA-crystallin was added to determine if it could prevent the heat-induced aggregation and precipitation of the βB1 protein as a molecular chaperone, a 1:1 molar ratio of αA-crystallin was less effectively chaperoned by the MU βB1 protein at 55 °C compared to the WT βB1 protein. This possibly implicates the mutation interrupts the interactions among crystallins which is crucial for lens transparency [49,50].

βB1-crystallin has long been known to be a crucial protein in forming heteromers with the acidic β-crystallins in the lens, and the formation of these heteromers is thought to be important to the maintenance of the transparency of the lens [51,52]. Thus, the novel p.Q227X mutation in this study might also result in ADCC via impairing the normal protein interactions and the stability of the heteromers with related crystallins. In this study, all affected individuals presented with nystagmus, which coincided with the clinical features in previously reported families with missense mutations located in the same domain in *CRYBB1* [14,26]. Traber et al. established an animal model for infantile nystagmus syndrome using albino mice, which could provide a powerful tool for exploring the mechanism of nystagmus resulting from the *CRYBB1* mutations in future research [53].

In summary, we have identified a novel heterozygous c. C749T (p.Q227X) mutation in *CRYBB1* in a family of Chinese origin with ADCC. Biophysical studies indicate that the mutation may lead to ADCC by modifying the structure of βB1-crystallin, inducing insolubility, and diminishing the thermal stability of the βB1-crystallin monomers or heteromers with αA-crystallin. Identification and characterization of this mutation further confirmed the importance of the C-terminal regions of βB1-crystallin in maintaining lens transparency which provides a novel insight into the molecular mechanism underlying the pathogenesis of human congenital cataract. Nevertheless, cataractogenesis is a complex process, much information remains to be elucidated in lens biology, and the genotype–phenotype relationship is not yet understood. Different mutations in the same gene can result in the same type of congenital cataract. However, the extremely variable morphologic characteristics of cataracts found in some families indicate that the same mutation in a single gene can result in different phenotypes. However, the accumulation of information about the mutation profiles and underlying molecular mechanism associated with the formation of inherited cataracts allow the emergence of new treatments and techniques for prevention. Moreover, it could be extended to age-related cataract in the future, which remains the leading cause of blindness worldwide.

APPENDIX 1. TWO-POINT LOD SCORES FOR LINKAGE BETWEEN CATARACT LOCUS AND CHROMOSOME 22 MARKERS.

To access the data, click or select the words "Appendix 1."

APPENDIX 2. THE REPORTED NONSENSE MUTATIONS IN CRYSTALLINE GENES.

To access the data, click or select the words "Appendix 2."

ACKNOWLEDGMENTS

This work was supported by the grants of Health and Family Planning Commission of Hubei Province (Grant No. WJ2015MB110) and the Program of the National Natural Science Foundation of China (Grant No. 81,472,024/H2005).

We thank the family for their involvement and Dr. Ming Yan for the contribution to the work as the co-corresponding author. The corresponding author emails are as following: zhengfang@whu.edu.cn (FZ); yanmingming1972@126.com (MY). The authors declare that they have no conflict of interest. AUTHOR CONTRIBUTION: Conceived and designed the experiments: FZ MY. Performed the experiment: YR GY. Analyzed the data: SD MY. Wrote the paper: FZ YR. Prepared the art: ZL CP.

REFERENCES

1. Shiels A, Hejtmancik JF. Molecular Genetics of Cataract. Prog Mol Biol Transl Sci 2015; 134:203-18. [PMID: 26310156].
2. Gilbert C, Foster A. Childhood blindness in the context of VISION 2020–the right to sight. Bull World Health Organ 2001; 79:227-32. [PMID: 11285667].
3. Apple DJ, Ram J, Foster A, Peng Q. Elimination of cataract blindness: a global perspective entering the new millenium. Surv Ophthalmol 2000; 45:Suppl 1S1-196. [PMID: 11291895].
4. Haargaard B, Wohlfahrt J, Rosenberg T, Fledelius HC, Melbye M. Risk factors for idiopathic congenital/infantile cataract. Invest Ophthalmol Vis Sci 2005; 46:3067-73. [PMID: 16123403].
5. Shiels A, Hejtmancik JF. Genetics of human cataract. Clin Genet 2013; 84:120-7. [PMID: 23647473].
6. Graw J. Genetics of crystallins: cataract and beyond. Exp Eye Res 2009; 88:173-89. [PMID: 19007775].
7. Messina-Baas O, Cuevas-Covarrubias SA. Inherited Congenital Cataract: A Guide to Suspect the Genetic Etiology in the Cataract Genesis. Mol Syndromol 2017; 8:58-78. [PMID: 28611546].
8. Augusteyn RC. On the growth and internal structure of the human lens. Exp Eye Res 2010; 90:643-54. [PMID: 20171212].
9. Willoughby CE, Shafiq A, Ferrini W, Chan LL, Billingsley G, Priston M, Mok C, Chandna A, Kaye S, Heon E. CRYBB1 mutation associated with congenital cataract and microcornea. Mol Vis 2005; 11:587-93. [PMID: 16110300].
10. Fernald RD, Wright SE. Maintenance of optical quality during crystalline lens growth. Nature 1983; 301:618-20. [PMID: 6828142].
11. Delaye M, Tardieu A. Short-range order of crystallin proteins accounts for eye lens transparency. Nature 1983; 302:415-7. [PMID: 6835373].
12. Campbell MC, Sands PJ. Optical quality during crystalline lens growth. Nature 1984; 312:291-2. [PMID: 6504144].
13. Cohen D, Bar-Yosef U, Levy J, Gradstein L, Belfair N, Ofir R, Joshua S, Lifshitz T, Carmi R, Birk OS. Homozygous CRYBB1 deletion mutation underlies autosomal recessive congenital cataract. Invest Ophthalmol Vis Sci 2007; 48:2208-13. [PMID: 17460281].
14. Wang J, Ma X, Gu F, Liu NP, Hao XL, Wang KJ, Wang NL, Zhu SQ. A missense mutation S228P in the CRYBB1 gene causes autosomal dominant congenital cataract. Chin Med J (Engl) 2007; 120:820-4. [PMID: 17531125].
15. Gu F, Zhai H, Li D, Zhao L, Li C, Huang S, Ma X. A novel mutation in major intrinsic protein of the lens gene (MIP) underlies autosomal dominant cataract in a Chinese family. Mol Vis 2007; 13:1651-6. [PMID: 17893667].
16. Chen Q, Ma J, Yan M, Mothobi ME, Liu Y, Zheng F. A novel mutation in CRYAB associated with autosomal dominant congenital nuclear cataract in a Chinese family. Mol Vis 2009; 15:1359-65. [PMID: 19597569].
17. Gu F, Luo W, Li X, Wang Z, Lu S, Zhang M, Zhao B, Zhu S, Feng S, Yan YB, Huang S, Ma X. A novel mutation in AlphaA-crystallin (CRYAA) caused autosomal dominant congenital cataract in a large Chinese family. Hum Mutat 2008; 29:769-[PMID: 18407550].
18. Chaves JM, Srivastava K, Gupta R, Srivastava OP. Structural and functional roles of deamidation and/or truncation of N- or C-termini in human alpha A-crystallin. Biochemistry 2008; 47:10069-83. [PMID: 18754677].
19. Srivastava K, Gupta R, Chaves JM, Srivastava OP. Truncated human betaB1-crystallin shows altered structural properties and interaction with human betaA3-crystallin. Biochemistry 2009; 48:7179-89. [PMID: 19548648].
20. Pang M, Su JT, Feng S, Tang ZW, Gu F, Zhang M, Ma X, Yan YB. Effects of congenital cataract mutation R116H on alphaA-crystallin structure, function and stability. Biochim Biophys Acta 2010; 1804:948-56. [PMID: 20079887].
21. Lampi KJ, Kim YH, Bachinger HP, Boswell BA, Lindner RA, Carver JA, Shearer TR, David LL, Kapfer DM. Decreased heat stability and increased chaperone requirement of modified human betaB1-crystallins. Mol Vis 2002; 8:359-66. [PMID: 12355063].
22. Eifert C, Burgio MR, Bennett PM, Salerno JC, Koretz JF. N-terminal control of small heat shock protein oligomerization: changes in aggregate size and chaperone-like function. Biochim Biophys Acta 2005; 1748:146-56. [PMID: 15769591].
23. Kundu M, Sen PC, Das KP. Structure, stability, and chaperone function of alphaA-crystallin: role of N-terminal region. Biopolymers 2007; 86:177-92. [PMID: 17345631].
24. Dolinska MB, Sergeev YV, Chan MP, Palmer I, Wingfield PT. N-terminal extension of beta B1-crystallin: identification of a critical region that modulates protein interaction with beta A3-crystallin. Biochemistry 2009; 48:9684-95. [PMID: 19746987].
25. Mackay DS, Boskovska OB, Knopf HL, Lampi KJ, Shiels A. A nonsense mutation in CRYBB1 associated with autosomal dominant cataract linked to human chromosome 22q. Am J Hum Genet 2002; 71:1216-21. [PMID: 12360425].

26. Wang KJ, Wang BB, Zhang F, Zhao Y, Ma X, Zhu SQ. Novel beta-crystallin gene mutations in Chinese families with nuclear cataracts. Arch Ophthalmol 2011; 129:337-43. [PMID: 21402992].

27. Yang J, Zhu Y, Gu F, He X, Cao Z, Li X, Tong Y, Ma X. A novel nonsense mutation in CRYBB1 associated with autosomal dominant congenital cataract. Mol Vis 2008; 14:727-31. [PMID: 18432316].

28. Wang KJ, Wang S, Cao NQ, Yan YB, Zhu SQ. A novel mutation in CRYBB1 associated with congenital cataract-microcornea syndrome: the p.Ser129Arg mutation destabilizes the betaB1/betaA3-crystallin heteromer but not the betaB1-crystallin homomer. Hum Mutat 2011; 32:E2050-60. [PMID: 21972112].

29. Ma AS, Grigg JR, Ho G, Prokudin I, Farnsworth E, Holman K, Cheng A, Billson FA, Martin F, Fraser C, Mowat D, Smith J, Christodoulou J, Flaherty M, Bennetts B, Jamieson RV. Sporadic and Familial Congenital Cataracts: Mutational Spectrum and New Diagnoses Using Next-Generation Sequencing. Hum Mutat 2016; 37:371-84. [PMID: 26694549].

30. Reis LM, Tyler RC, Muheisen S, Raggio V, Salviati L, Han DP, Costakos D, Yonath H, Hall S, Power P, Semina EV. Whole exome sequencing in dominant cataract identifies a new causative factor, CRYBA2, and a variety of novel alleles in known genes. Hum Genet 2013; 132:761-70. [PMID: 23508780].

31. Khan AO, Aldahmesh MA, Mohamed JY, Alkuraya FS. Clinical and molecular analysis of children with central pulverulent cataract from the Arabian Peninsula. Br J Ophthalmol 2012; 96:650-5. [PMID: 22267527].

32. Meyer E, Rahman F, Owens J, Pasha S, Morgan NV, Trembath RC, Stone EM, Moore AT, Maher ER. Initiation codon mutation in betaB1-crystallin (CRYBB1) associated with autosomal recessive nuclear pulverulent cataract. Mol Vis 2009; 15:1014-9. [PMID: 19461930].

33. Pras E, Frydman M, Levy-Nissenbaum E, Bakhan T, Raz J, Assia EI, Goldman B, Pras E. A nonsense mutation (W9X) in CRYAA causes autosomal recessive cataract in an inbred Jewish Persian family. Invest Ophthalmol Vis Sci 2000; 41:3511-5. [PMID: 11006246].

34. Devi RR, Yao W, Vijayalakshmi P, Sergeev YV, Sundaresan P, Hejtmancik JF. Crystallin gene mutations in Indian families with inherited pediatric cataract. Mol Vis 2008; 14:1157-70. [PMID: 18587492].

35. Santana A, Waiswol M, Arcieri ES, de Vasconcellos JPC, de Melo MB. Mutation analysis of CRYAA, CRYGC, and CRYGD associated with autosomal dominant congenital cataract in Brazilian families. Mol Vis 2009; 15:793-800. [PMID: 19390652].

36. Yang GX, Chen ZM, Zhang WL, Liu ZQ, Zhao JL. Novel mutations in CRYGD are associated with congenital cataracts in Chinese families. Sci Rep 2016; •••:6-[PMID: 26732753].

37. Hansen L, Yao W, Eiberg H, Kjaer KW, Baggesen K, Hejtmancik JF, Rosenberg T. Genetic heterogeneity in microcornea-cataract: five novel mutations in CRYAA, CRYGD, and GJA8. Invest Ophthalmol Vis Sci 2007; 48:3937-44. [PMID: 17724170].

38. Zhai Y, Li J, Zhu Y, Xia Y, Wang W, Yu Y, Yao K. A nonsense mutation of gammaD-crystallin associated with congenital nuclear and posterior polar cataract in a Chinese family. Int J Med Sci 2014; 11:158-63. [PMID: 24465161].

39. Zhuang X, Wang L, Song Z, Xiao W. A Novel Insertion Variant of CRYGD Is Associated with Congenital Nuclear Cataract in a Chinese Family. PLoS One 2015; 10:e0131471-[PMID: 26147294].

40. Santhiya ST, Shyam Manohar M, Rawlley D, Vijayalakshmi P, Namperumalsamy P, Gopinath PM, Loster J, Graw J. Novel mutations in the gamma-crystallin genes cause autosomal dominant congenital cataracts. J Med Genet 2002; 39:352-8. [PMID: 12011157].

41. Zhang LY, Yam GH, Fan DS, Tam PO, Lam DS, Pang CP. A novel deletion variant of gammaD-crystallin responsible for congenital nuclear cataract. Mol Vis 2007; 13:2096-104. [PMID: 18079686].

42. Yao K, Jin C, Zhu N, Wang W, Wu R, Jiang J, Shentu X. A nonsense mutation in CRYGC associated with autosomal dominant congenital nuclear cataract in a Chinese family. Mol Vis 2008; 14:1272-6. [PMID: 18618005].

43. Li D, Wang S, Ye H, Tang Y, Qiu X, Fan Q, Rong X, Liu X, Chen Y, Yang J, Lu Y. Distribution of gene mutations in sporadic congenital cataract in a Han Chinese population. Mol Vis 2016; 22:589-98. [PMID: 27307692].

44. Gillespie RL, O'Sullivan J, Ashworth J, Bhaskar S, Williams S, Biswas S, Kehdi E, Ramsden SC, Clayton-Smith J, Black GC, Lloyd IC. Personalized diagnosis and management of congenital cataract by next-generation sequencing. Ophthalmology 2014; •••:1212124-37. [PMID: 25148791].

45. Guo Y, Su D, Li Q, Yang Z, Ma Z, Ma X, Zhu S. A nonsense mutation of CRYGC associated with autosomal dominant congenital nuclear cataracts and microcornea in a Chinese pedigree. Mol Vis 2012; 18:1874-80. [PMID: 22876111].

46. Zhang L, Fu SB, Ou YS, Zhao TT, Su YJ, Liu P. A novel nonsense mutation in CRYGC is associated with autosomal dominant congenital nuclear cataracts and microcornea. Mol Vis 2009; 15:276-82. [PMID: 19204787].

47. Khajavi M, Inoue K, Lupski JR. Nonsense-mediated mRNA decay modulates clinical outcome of genetic disease. Eur J Hum Genet 2006; 14:1074-81. [PMID: 16757948].

48. Holbrook JA, Neu-Yilik G, Hentze MW, Kulozik AE. Nonsense-mediated decay approaches the clinic. Nat Genet 2004; 36:801-8. [PMID: 15284851].

49. Liu BF, Liang JJ. Interaction and biophysical properties of human lens Q155* betaB2-crystallin mutant. Mol Vis 2005; 11:321-7. [PMID: 15889016].

50. Takemoto L, Sorensen CM. Protein-protein interactions and lens transparency. Exp Eye Res 2008; 87:496-501. [PMID: 18835387].

51. Ajaz MS, Ma Z, Smith DL, Smith JB. Size of human lens beta-crystallin aggregates are distinguished by N-terminal truncation of betaB1. J Biol Chem 1997; 272:11250-5. [PMID: 9111027].

52. Chan MP, Dolinska M, Sergeev YV, Wingfield PT, Hejtmancik JF. Association properties of betaB1- and betaA3-crystallins: ability to form heterotetramers. Biochemistry 2008; 47:11062-9. [PMID: 18823128].

53. Traber GL, Chen CC, Huang YY, Spoor M, Roos J, Frens MA, Straumann D, Grimm C. Albino mice as an animal model for infantile nystagmus syndrome. Invest Ophthalmol Vis Sci 2012; 53:5737-47. [PMID: 22789924].

Articles are provided courtesy of Emory University and the Zhongshan Ophthalmic Center, Sun Yat-sen University, P.R. China. The print version of this article was created on 1 September 2017. This reflects all typographical corrections and errata to the article through that date. Details of any changes may be found in the online version of the article.